Donor-acceptor based two-dimensional covalent organic frameworks for near-infrared photothermal conversion

Yue Zhang,[a] Guiyuan Wu,[b] Hui Liu,[a] Rui Tian,[a] Yan Li,[a] Danbo Wang,[a] Renzeng Chen,[a] Jinyu Zhao,[a] Shipeng Liu,[a] Zhibo Li,*[a,c] and Yingjie Zhao*[a]

[a] *College of Polymer Science and Engineering, Qingdao University of Science and Technology, Qingdao 266042, China*

[b] *Anhui Province Key Laboratory of Optoelectronic Material Science and Technology, School of Physics and Electronic Information, Anhui Normal University, Wuhu, 241002, China*

[c] *College of Chemical Engineering, Qingdao University of Science and Technology, Qingdao 266042, China*

[*] Corresponding Authors: zbli@qust.edu.cn; yz@qust.edu.cn

Supporting Information

Table of Contents

1. Supporting Methods

1.1. General materials and methods

Unless otherwise specified, all other reagents were purchased commercially and used as received. Organic reagents including ethanol, dichloromethane (DCM), petroleum ether (PE), N,N-dimethylformamide (DMF), 1,4-dioxane, acetic acid, 4-formylbenzeneboronic acid pinacol ester were purchased from Adamas; 1,2-dichlorobenzene, tris(4-aminophenyl)amine were purchased from Alfa Aesar; sulfuric acid was purchased from Yantai Far East Fine Chemical Co., Ltd; *n*-octylamine, 1,4,5,8-naphthalenetetracarboxylic dianhydride, 1,3-dibromo-5,5-dimethylhydantoin (DBH), tetrakis(triphenylphosphine)palladium ($Pd(PPh_3)_4$), 1,3,5-tris(4-aminophenyl)benzene were purchased from Energy Chemical; mesitylene was purchased from J&K Scientific; sodium carbonate was purchased from Shanghai Titan Scientific Co., Ltd. Nitrogen stored in the high-pressure gas cylinder was ordered from Dehai Gas, Qingdao. Tetrahydrofuran (THF) were redistilled under argon reflux with Na crumbs. All aqueous solutions were prepared with Milli-Q water.

All reactions were carried out under nitrogen condition unless otherwise noted. Column chromatography was carried out on silica gel (200 - 300 mesh). TLC analysis was performed on precoated silica gel plates (0.2 mm thick). ^{1}H and ^{13}C NMR spectra were performed on 400 MHz spectrometers (Bruker AVANCE NEO 400 Ascend) in the indicated solvents at room temperature. High resolution solid-state NMR spectra were recorded on Agilent NMR Spectrometer (600 - 54 - ASC) using a standard CP

pulse sequence probe with 4 mm (outside diameter) zirconia rotors. Attenuated total reflectance (ATR) FT-IR spectra were recorded on a Bruker Tensor 27 Spectrometer. TGA from 40 - 800 °C was carried out on an American TA-Q20 in nitrogen 3 atmosphere using a 10 °C/min ramp without equilibration delay. MALDI-TOF mass spectrometry analysis was performed on a Bruker Microflex-LRF mass spectrometer in positive ion. Scanning electron microscope (SEM) images were collected using scanning electron microscope (JEOL, JSM-7500F) at an accelerating voltage of 5.0 kV. Transmission electron microscope (TEM) were performed on a JEM-2100 electron microscope with an accelerating voltage of 200 kV. The Solid-state UV-Vis absorbance were measured by UV spectrophotometer (HITACHI, U-3900). Powder X-ray diffraction (PXRD) patterns were obtained on a PANalytical Empyrean X-Ray diffractometer with Cu Kα line focused radiation at 40 kV and 40 mA from 2θ = 1.5° up to 30° with 0.02° increment by Bragg-Brentano. The powdered sample was added to the glass and compacted for measurement. N_2 adsorption isotherms were measured up to 1 bar at 77 K using a Micrometrics ASAP 2460 surface area analyzer. Prior to measurements, samples (ca. 50 mg) were degassed for over 12 h at 120 °C. UHP grade N_2 and He were used throughout the adsorption experiments. Oil-free vacuum pumps and oil-free pressure regulators were used for measurements to prevent contamination of the samples during the degassing process and isotherm measurement. Cyclic voltammetry (CV) was performed using a standard one compartment, threeelectrode electrochemical cell attached to an CHI 760E Electrochemical Workstation. The Ag/AgCl aqueous electrode was used as reference electrode. Glass-carbon was used as

the working electrode, and Pt was used as the counter electrode. Tetrabutylammonium hexafluorophosphate (0.1 M) in dichloromethane was used as electrolyte. The potential range was set between - 2.4 V and 0.0 V and the scan rate was 100 mV s^{-1}.

1.2 Synthesis

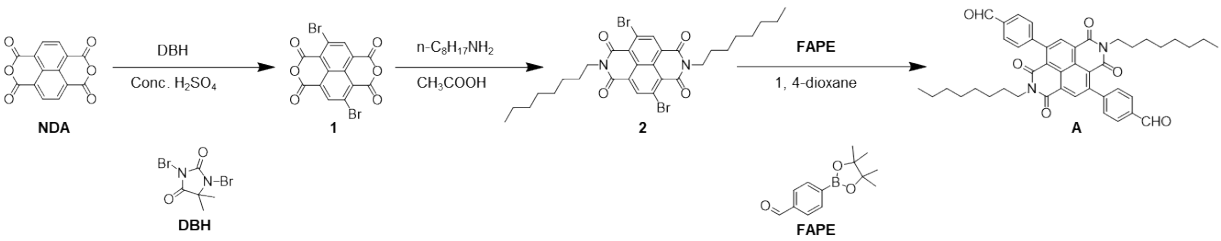

Compound 1. This compound was prepared following the literature procedure.[1]

Compound 2. This compound was prepared following the literature procedure.[1]

Compound A. A mixture of 2 M Na_2CO_3 in H_2O (15 mL) and 1,4-dioxane (80 mL) was degassed by bubbling N_2 for 30 min. Then compound **2** (1.00 g, 1.54 mmol), FAPE (1.44 g, 6.20 mmol) and $Pd(PPh_3)_4$ (0.18 g, 0.16 mmol) were added into the mixture. The reaction mixture was then heated up to 110 °C under N_2 nitrogen atmosphere for 24 h. Then DCM was added into the mixture for dilution, and the organic layer was washed consecutively with water and brine before being dried over Na_2SO_4 and concentrated. The crude product was then purified by column chromatography flash silica gel, with DCM : PE (1 : 1) as eluent to afford target product (yellow solid, 334 mg, 31 %); ^{1}H NMR (400 MHz, $CDCl_3$): 10.15 (s, 2H), 8.64 (s, 2H), 8.10–8.03 (m, 4H), 7.57 (d, J = 8.1 Hz, 4H), 4.09 - 4.03 (m, 4H), 1.67 - 1.59 (m, 4H), 1.27 (d, J = 11.7 Hz, 20H), 0.86 (d, J = 6.5 Hz, 6H); ^{13}C NMR (101 MHz, $CDCl_3$): 190.65, 161.06,

145.50, 134.88, 134.05, 128.79, 127.66, 126.31, 124.89, 122.12, 40.12, 30.72, 28.17, 26.96, 25.98, 21.58, 13.04.

PT-N-COF. By condensing block A (30 mg, 0.043 mmol) and tris(4-aminophenyl)amine (8 mg, 0.029 mmol) in the mixture of 1,2-dichlorobenzene/mesitylene/acetic acid (9:1:1, by volume) at 120 °C for 72 h, **PT-N-COF** was isolated as green powder insoluble in common organic solvents (^{13}C CP/MAS spectra shown as Figure S1).

PT-B-COF. By condensing block A (30 mg, 0.043 mmol) and 1,3,5-Tris(4-aminophenyl)benzene (10 mg, 0.029 mmol) in the mixture of 1,2-dichlorobenzene/mesitylene/acetic acid (5:5:1, by volume) at 120 °C for 72 h, **PT-B-COF** was isolated as red powder insoluble in common organic solvents (^{13}C CP/MAS spectra shown as Figure S2).

1.3 Photothermal conversion properties measurement

COFs powders were put in a cuvette and covered bottom. The 808 nm laser beam (Hi-Tech Optoelectronics Co., Ltd, Beijing, China) irradiated at a power density of 1.8 W/cm^2. And the temperature was measured with an IR thermal camera (FLUKE TiS_20 Thermal Imaging Camera). The calculation of PT conversion efficiency was determined according to the previous methods (see section 1.4).

1.4 Calculation of the photothermal conversion efficiency

The conversion efficiency was determined according to the previous method.[2] Details are as follows:

Based on the total energy balance for this system:

$$\sum_i m_i C_{pi} \frac{dT}{dt} = Q_s - Q_{loss}$$

where m_i and $C_{p,i}$ are the mass and heat capacity of system components (COFs samples and substrate), respectively. Q_s is the photothermal heat energy input by irradiating NIR laser to COFs samples, and Q_{loss} is thermal energy lost to the surroundings. When the temperature is maximum, the system is in balance.

$$Q_s = Q_{loss} = hS\Delta T_{max}$$

where h is the heat transfer coefficient, S is the surface area of the container, ΔT_{max} is the maximum temperature change. The photothermal conversion efficiency η is calculated from the following equation:

$$\eta = \frac{hS\Delta T_{max}}{I\left(1 - 10^{-A_{808}}\right)}$$

where I is the laser power (1.8 W/cm^2) and A_{808} is the absorbance of the samples at the wavelength of 808 nm.

In order to obtain the *hS*, a dimensionless driving force temperature, θ is introduced as follows:

$$\theta = \frac{T - T_{surr}}{T_{max} - T_{surr}}$$

where T is the temperature of COFs samples, T_{max} is the maximum system temperature, and T_{surr} is the initial temperature (28 °C).

The sample system time constant τ_s

$$\tau_s = \frac{\sum_i m_i C_{p,i}}{hS}$$

thus $\frac{d\theta}{dt} = \frac{1}{\tau_s hS\Delta T_{max}} Q_s - \frac{\theta}{\tau_s}$

when the laser is off, $Q_s = 0$, therefore $\frac{d\theta}{dt} = -\frac{\theta}{\tau_s}$, and $t = -\tau_s \ln\theta$

so *hS* could be calculated from the slope of cooling time vs ln θ. Therefore, τ_s of **PT-N-COF** and **PT-B-COF** are 17.26 s and 29.98 s (Figure S7, S8), the photothermal conversion efficiency η of **PT-N-COF** and **PT-B-COF** are 66.4 % and 31.2 %, respectively. **PT-N-COF** and **PT-B-COF**

	m_i (g)	$C_{p,i}$ (J (g °C)$^{-1}$)	T_{max} (℃)	τ_s (s)	η
PT-N-COF	0.5	0.50	94	17.26	66.4 %
PT-B-COF	0.5	0.61	43	29.98	31.2 %

1.5 Structural simulation

Structural modeling of **PT-N-COF** and **PT-B-COF** was performed in the Materials Studio 7.0 software package. The space groups were obtained from the Reticular Chemistry Structure Resource. P6 was chosen for AA. The theoretical models were then optimized by the Forcite module.

Pawley refinements of the PXRD patterns were done in the Reflex module using data from 1 to 30°. The integrated intensities were extracted using Pseudo-Voigt profile. The unit cell parameters a, b, c, FWHM parameters U, V, W, profile parameters NA, NB, and zero point were refined. The background was refined with 20th order polynomial.

1.6 References

1. M. Sasikumar, Y. V. Suseela and T. Govindaraju, *Asian J. Org. Chem.*, 2013, **2**, 779-785.
2. Y. Cao, J.-H. Dou, N.-j. Zhao, S. Zhang, Y.-Q. Zheng, J.-P. Zhang, J.-Y. Wang, J. Pei and Y. Wang, *Chem. Mater.*, 2017, **29**, 718-725.

2. Supporting Figures and Legends

Space group	P6		
Calculated unit cell	a = b = 50.4013 Å, c = 4.2408 Å and α = β = 90°, γ = 120°		
Atom	x	y	z
C	0.18725	-0.38315	0.9134
C	0.99244	-0.44318	0.74409
C	0.0081	-0.45982	0.75905
C	0.99184	-0.49182	0.76825
C	0.95922	-0.50775	0.76111
C	0.94461	-0.49003	0.7169
C	0.04017	-0.44413	0.76616
C	0.05714	-0.45931	0.77376
O	0.91759	-0.5026	0.64522
O	0.00708	-0.41551	0.72498
C	0.08949	-0.44065	0.80939
N	0.03927	-0.54162	0.73983
C	0.05753	-0.55752	0.73217
C	0.10594	-0.44861	1.02015
C	0.13763	-0.43028	1.05447
C	0.15368	-0.40263	0.88785
C	0.13742	-0.39364	0.6889
C	0.10581	-0.4123	0.65012
C	0.69983	-0.65344	1.20036
C	0.71315	-0.66781	1.0305
C	0.74489	-0.65422	1.00056
C	0.76434	-0.62555	1.13948

C	0.75134	-0.61164	1.3182
C	0.71956	-0.62535	1.34837
N	0.79708	-0.6094	1.10025
C	0.95808	-0.40975	0.86885
C	0.93461	-0.39952	0.93564
C	0.95041	-0.36639	1.05513
C	0.92695	-0.35624	1.12376
C	0.94276	-0.32303	1.24067
C	0.9193	-0.31292	1.31025
C	0.93496	-0.27986	1.42651
H	0.19843	-0.36312	0.76442
H	0.05216	-0.41937	0.78236
H	0.07876	-0.5438	0.8732
H	0.06491	-0.55778	0.48628
H	0.09417	-0.46911	1.15985
H	0.14945	-0.43761	1.2147
H	0.14929	-0.37244	0.55703
H	0.09445	-0.40506	0.483
H	0.69907	-0.68954	0.91782
H	0.75371	-0.66632	0.8663
H	0.76593	-0.5897	1.42935
H	0.71045	-0.6134	1.4787
H	0.9748	-0.39353	0.69487
H	0.97014	-0.40881	1.09155
H	0.91798	-0.41483	1.11595
H	0.92181	-0.40135	0.71567
H	0.9669	-0.35101	0.87416

H	0.96335	-0.36452	1.27413
H	0.91055	-0.3715	1.30603
H	0.91389	-0.35827	0.90516
H	0.9591	-0.30776	1.05806
H	0.95588	-0.32098	1.4589
H	0.90295	-0.32802	1.49355
H	0.90613	-0.31482	1.09289
H	0.95066	-0.26414	1.24284
H	0.94823	-0.27731	1.64452
H	0.9174	-0.27334	1.47971
N	0.33333	-0.33333	1.21235

Table S1. Unit cell parameters and fractional atomic coordinates for **PT-N-COF** based AA topology after unit cell correction and Pawley refinement.

Space group	P6		
Calculated unit cell	a = b = 56.2682 Å, c = 4.1686 Å and α = β = 90°, γ = 120°		
Atom	x	y	z
C	1.63654	0.27389	0.84683
C	1.61218	0.25932	0.66908
C	1.59765	0.23062	0.6707
C	1.6071	0.21586	0.84697
C	1.63162	0.23033	1.02281
C	1.64607	0.25905	1.02403
N	1.59133	0.18641	0.83477
C	1.65197	0.30442	0.84685
C	1.68079	0.31891	0.84682
C	1.59538	0.16912	0.99925
C	1.44945	0.00737	0.83397
C	1.47754	0.01553	0.84262
C	1.48569	0.99586	0.84916
C	1.46544	0.96752	0.83847
C	1.43766	0.96081	0.79407
C	1.49745	0.04346	0.84549
C	1.52574	0.05277	0.84703
O	1.42046	0.93783	0.71017
O	1.44289	0.02493	0.82085
C	1.54364	0.08167	0.87564
N	1.57019	0.02002	0.82816
C	1.6003	0.03035	0.82794
C	1.60962	0.01078	0.96169

C	1.64061	0.02604	1.02799
C	1.64994	0.0062	1.14548
C	1.68087	0.0214	1.212
C	1.69021	0.00151	1.32734
C	1.56631	0.09275	1.08478
C	1.5832	0.1211	1.12038
C	1.5774	0.13927	0.95558
C	1.55444	0.1286	0.75336
C	1.5378	0.10026	0.71395
C	1.72112	0.01671	1.39475
C	1.26938	0.00324	1.51015
H	1.60478	0.27008	0.52119
H	1.5791	0.21963	0.52964
H	1.63965	0.21977	1.16223
H	1.66433	0.26966	1.17078
H	1.69177	0.30771	0.84672
H	1.61181	0.17605	1.17231
H	1.49057	0.05833	0.86229
H	1.61048	0.04927	0.97802
H	1.60837	0.03663	0.58085
H	1.60521	0.99447	0.7824
H	1.59841	0.00116	1.18744
H	1.64568	0.04214	1.21264
H	1.65186	0.03625	0.80441
H	1.645	0.99014	0.96053
H	1.63866	0.99589	1.3685
H	1.68582	0.03737	1.39802

H	1.69214	0.03175	0.98911
H	1.68532	0.98557	1.14106
H	1.6789	0.9911	1.54984
H	1.57075	0.0795	1.22702
H	1.60039	0.12881	1.28468
H	1.54971	0.14222	0.61981
H	1.52107	0.09299	0.5436
H	1.72613	0.03263	1.58145
H	1.73259	0.02709	1.17292
H	1.24706	0.99166	1.56364
H	1.2732	0.01875	1.32239
H	1.28056	0.01393	1.73165

Table S2. Unit cell parameters and fractional atomic coordinates for **PT-B-COF** based AA topology after unit cell correction and Pawley refinement.

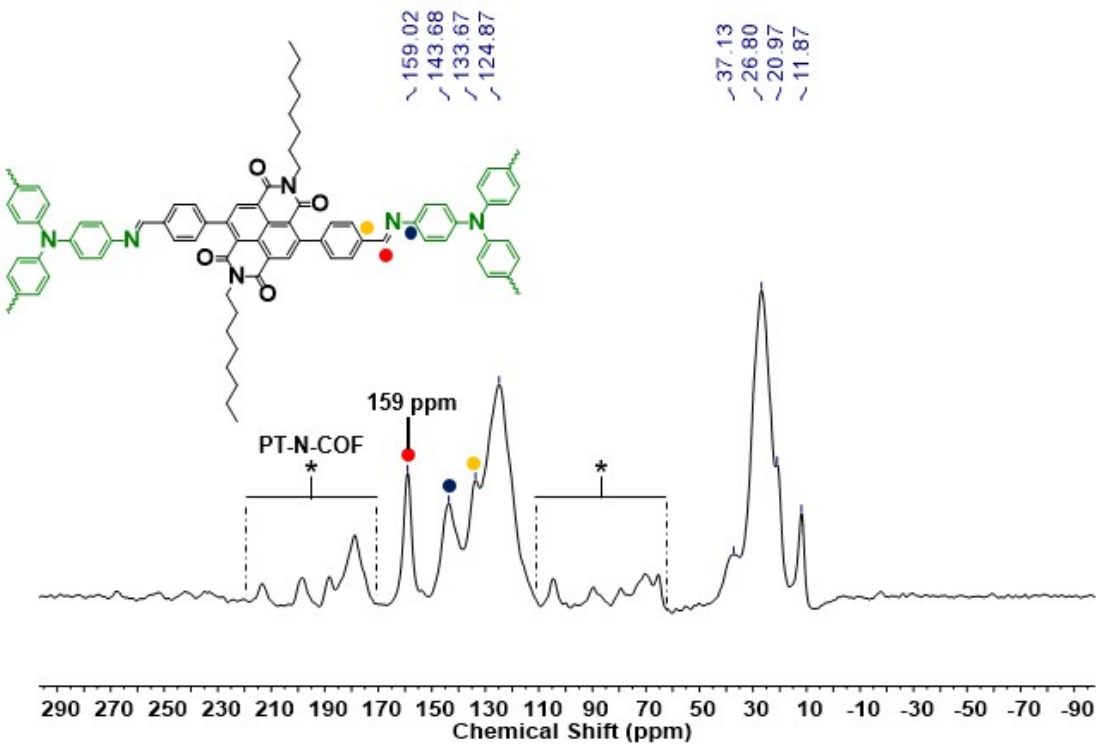

Figure S1. ^{13}C CP/MAS (150 MHz) spectrum of **PT-N-COF**. Spinning sidebands are marked with asterisk (*).

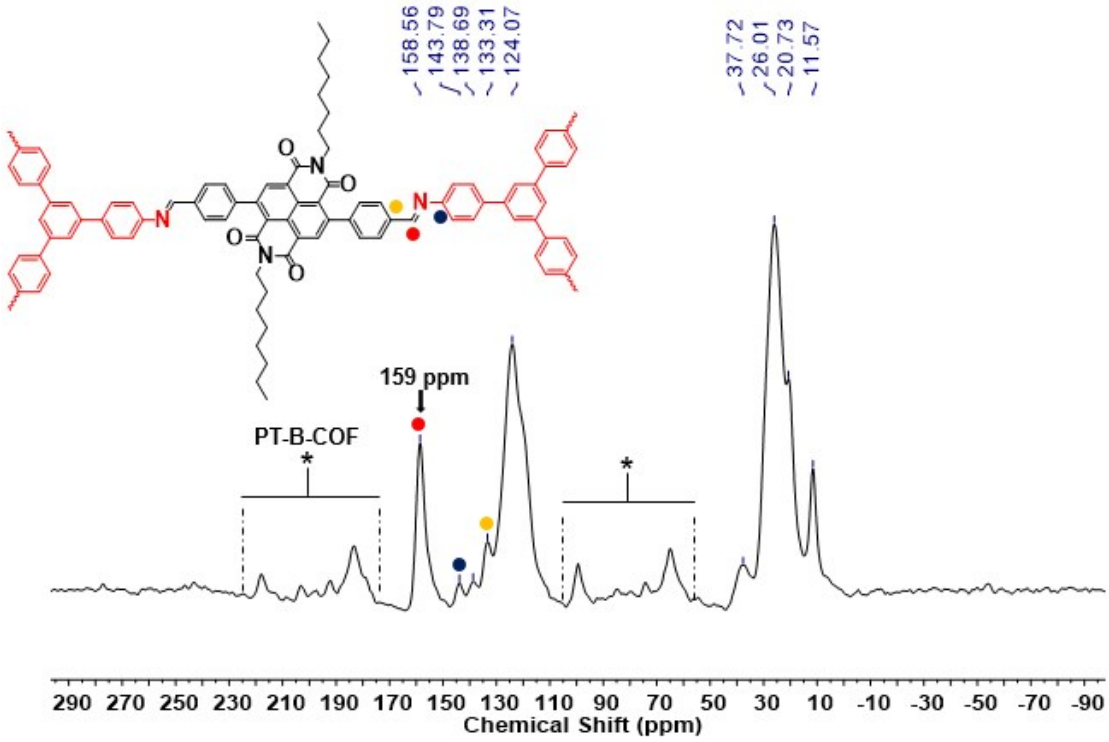

Figure S2. ^{13}C CP/MAS (150 MHz) spectrum of **PT-B-COF**. Spinning side bands are marked with asterisk (*).

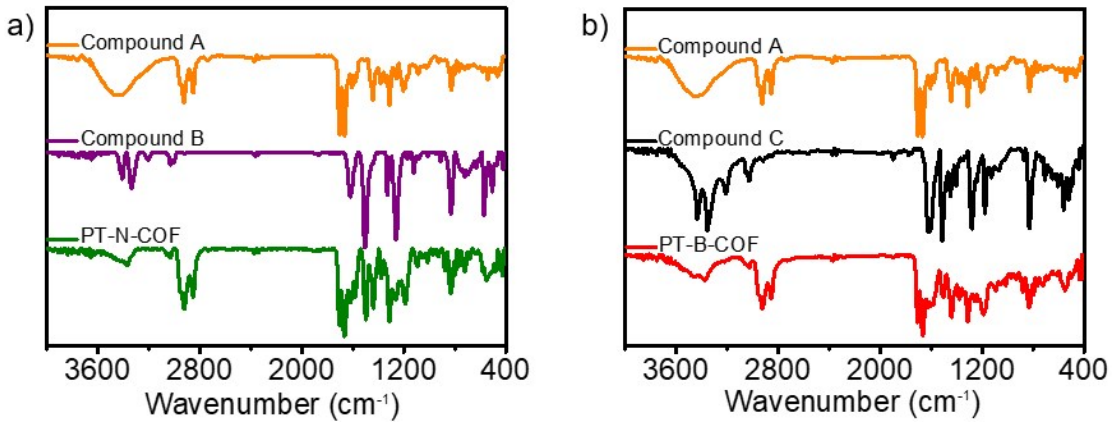

Figure S3. The FT-IR spectra of (a) compound **A**, compound **B**, **PT-N-COF** and (b) compound **A**, compound **C**, **PT-B-COF**.

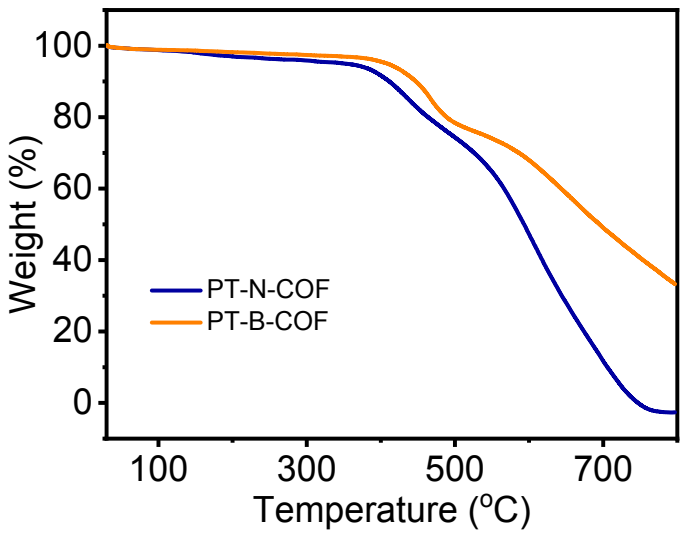

Figure S4. The thermogravimetric analysis (TGA) profiles of **PT-N-COF** and **PT-B-COF**.

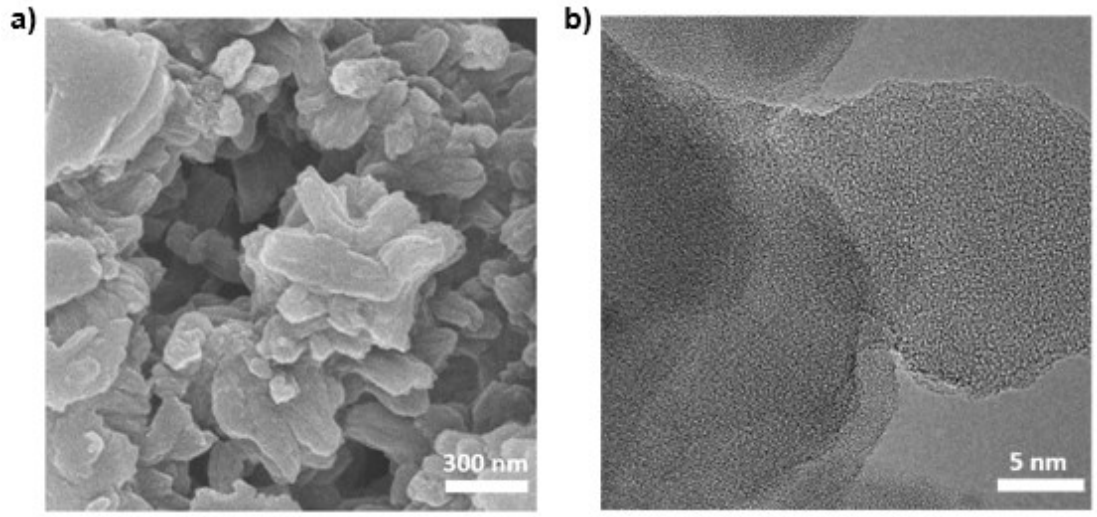

Figure S5. (a) SEM image of **PT-N-COF**; (b) TEM image of **PT-N-COF**.

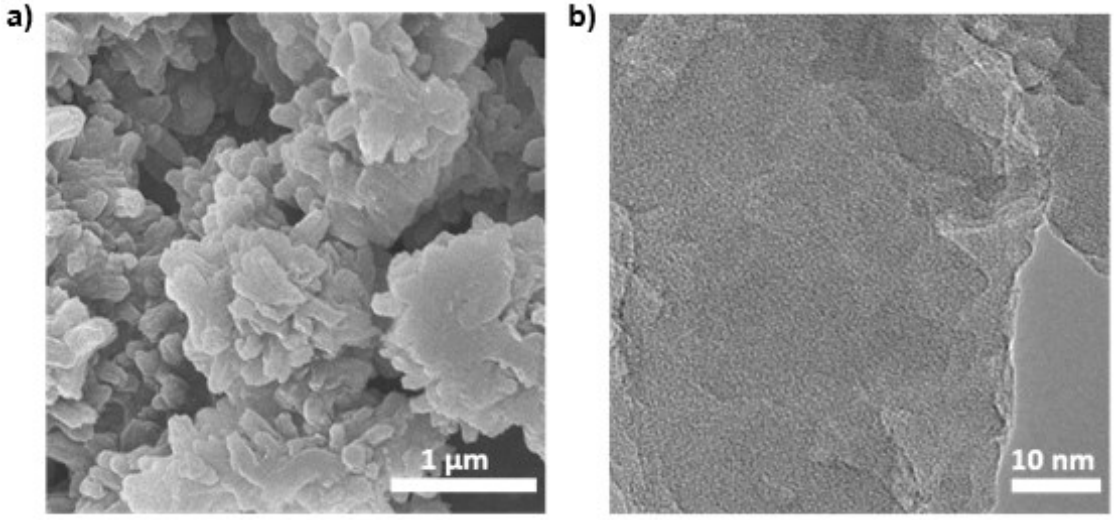

Figure S6. (a) SEM image of **PT-B-COF**; (b) TEM image of **PT-B-COF**.

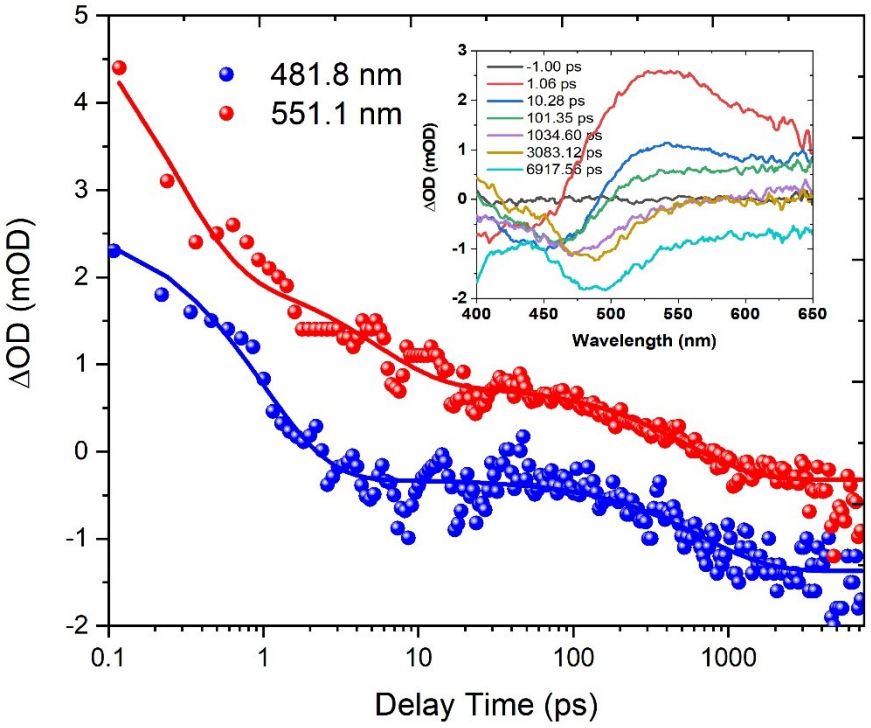

Figure S7. The femtosecond dynamics of **PT-N-COF** at 481.8 nm and 551.1 nm. The corresponding spectra at different selected delay times were shown in the inserted picture.

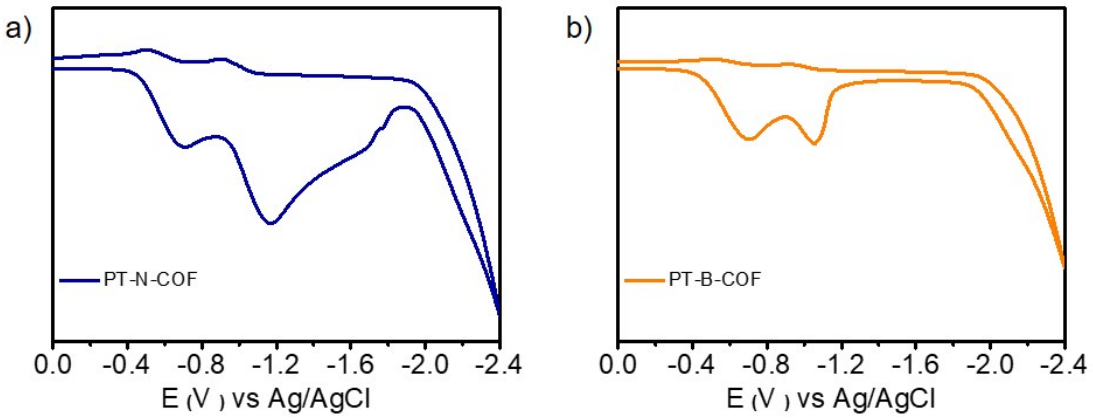

Figure S8. Cyclic voltammograms of (a) **PT-N-COF** and (b) **PT-B-COF** in dichloromethane at 298 K.

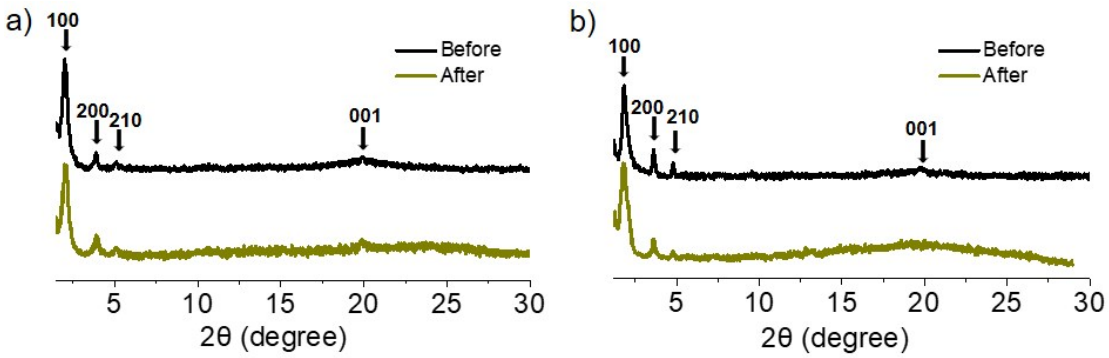

Figure S9. PXRD profiles of (a) **PT-N-COF** and (b) **PT-B-COF** before/after photothermal conversion properties measurement.

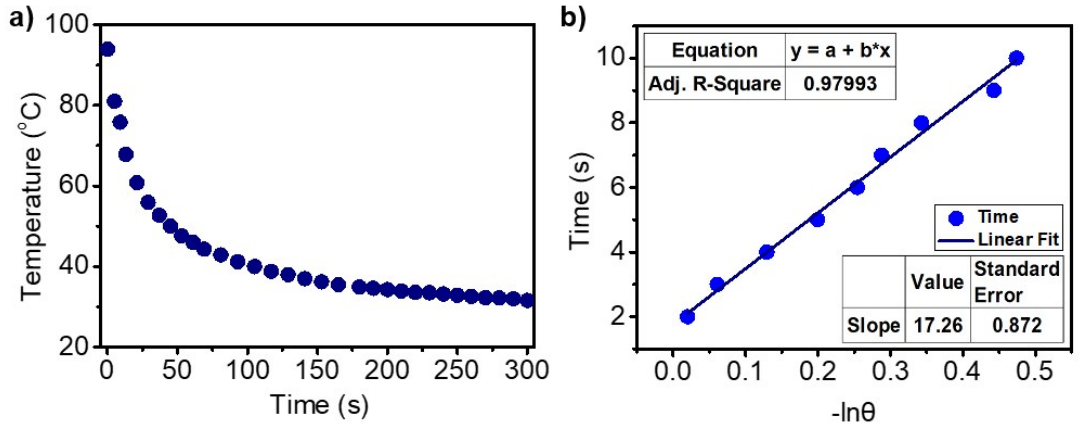

Figure S10. (a) The cooling curve of **PT-N-COF** after irradiation with 808 nm laser (1.8 W/cm^2); (b) A linear fitting correlation between time (t) and -ln θ obtained from the cooling period in Figure S7 (a).

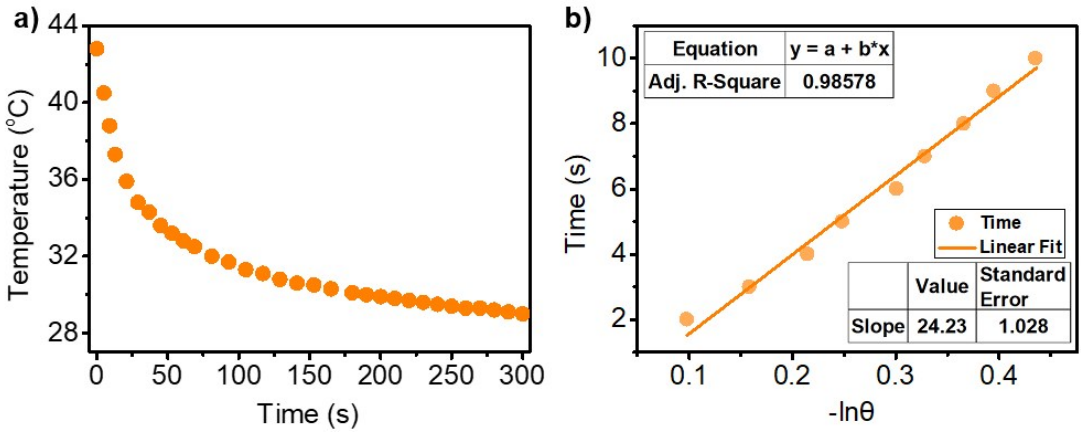

Figure S11. (a) The cooling curve of **PT-B-COF** after irradiation with 808 nm laser (1.8 W/cm^2); (b) A linear fitting correlation between time (t) and -ln θ obtained from the cooling period in Figure S8 (a).

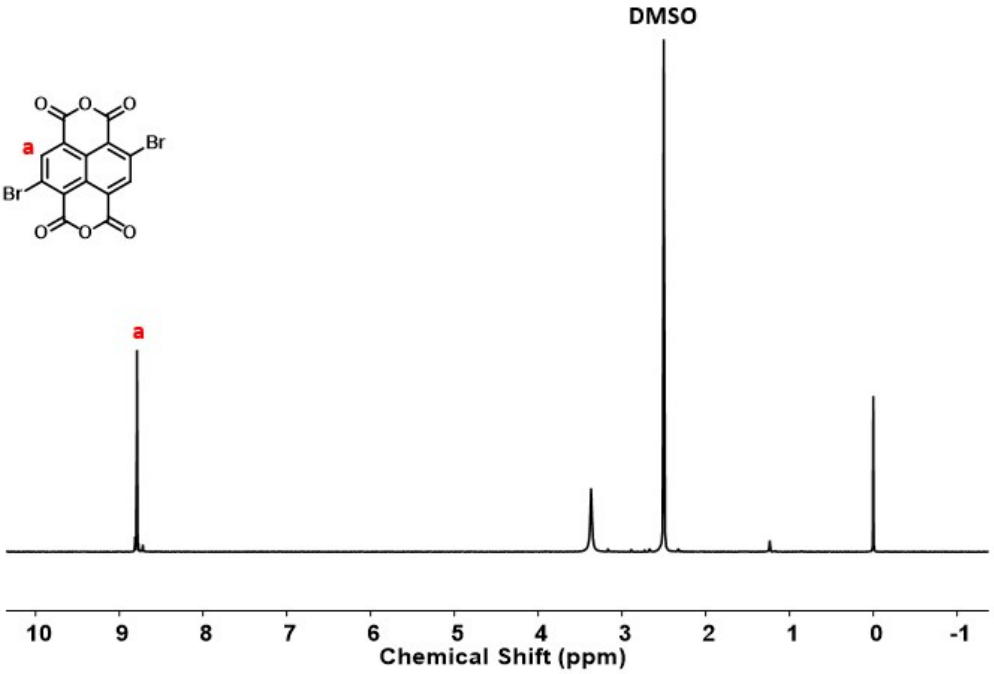

Figure S12. ^{1}H NMR (400 MHz) spectrum of compound **1** in DMSO.

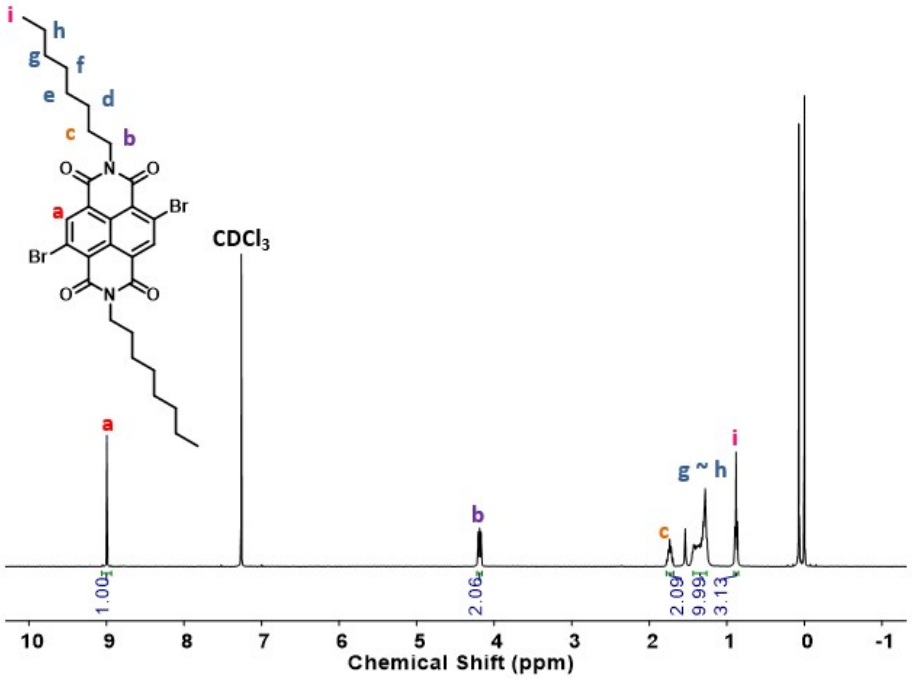

Figure S13. ^{1}H NMR (400 MHz) spectrum of compound **2** in $CDCl_3$.

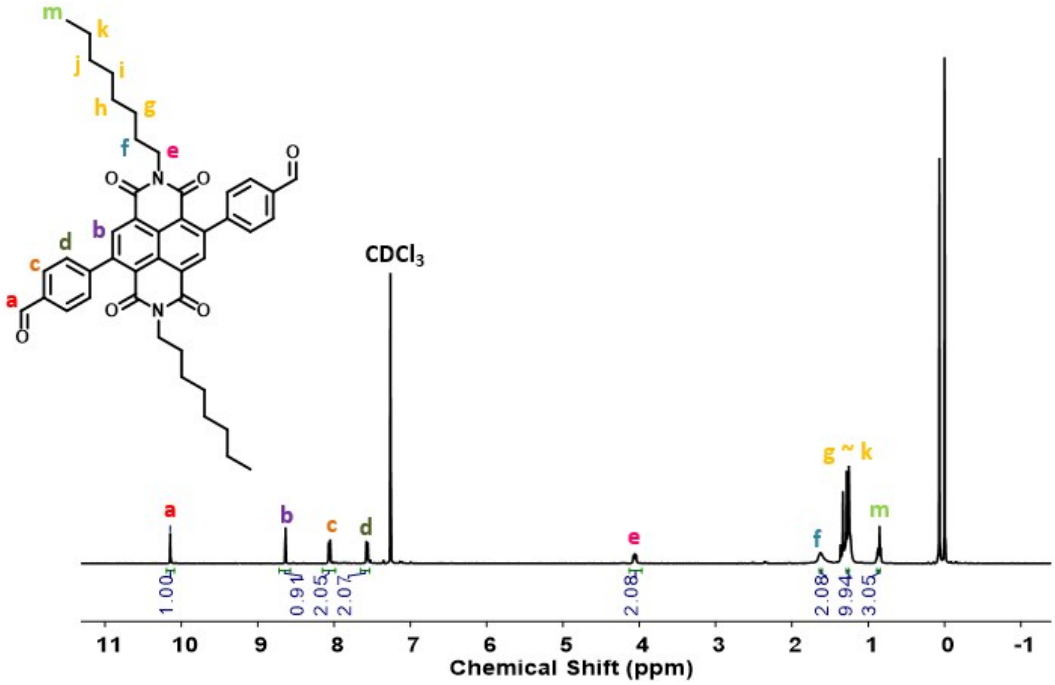

Figure S14. ^{1}H NMR (400 MHz) spectrum of compound **A** in $CDCl_3$.

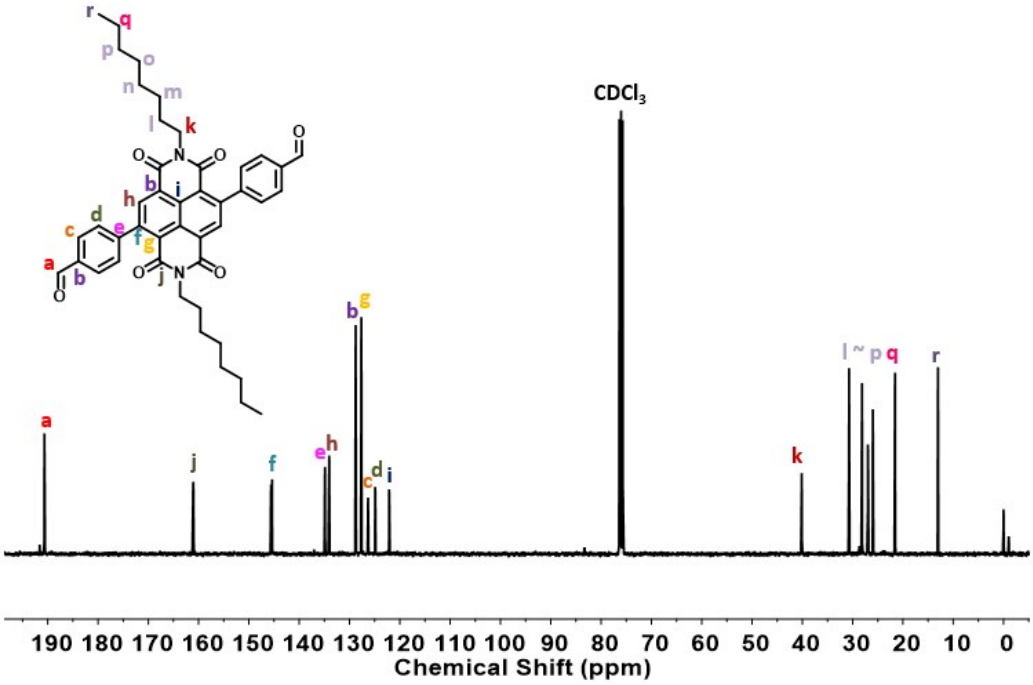

Figure S15. ^{13}C NMR (101 MHz) spectrum of compound **A** in $CDCl_3$.